Investigation of BURLE 8854 Photomultiplier Tube

M. Shepherd
Indiana University,
Thomas Jefferson National Accelerator Facility

A. Pope
Carnegie Mellon University,
Thomas Jefferson National Accelerator Facility

August 26, 1997

1 Abstract

The purpose of this research was to investigate the behavior of the BURLE 8854 Photomultiplier tube used extensively for detectors of Cherenkov radiation in the Hall A Spectrometers at Thomas Jefferson National Accelerator Facility (CEBAF). A study of how supply voltage effects the overall efficiency of the phototube was conducted. In particular, it was necessary to investigate whether or not increasing the applied voltage to the phototube increases the efficiency at which it detects light. An investigation of the linearity of the phototube was also conducted. This involved trying to find how much charge the phototube, in conjunction with the current base, is capable of producing. Finally, a Monte Carlo simulation of the phototube and base was created to aid in examining the relationship between the average number of photoelectrons produced at the photocathode and the charge spectrum observed.

Quantum Efficiency at 385 nm	22.5%
Maximum Anode to Cathode Voltage	3000 V
Maximum Average Anode Current	200 μA
Linear Pulse Current	0.13 A
Typical Current Gain	5.1×10^7
Typical Rise Time	4 ns
Typical Transit Time	78 ns

Figure 1: Published Data[1] on the BURLE 8854

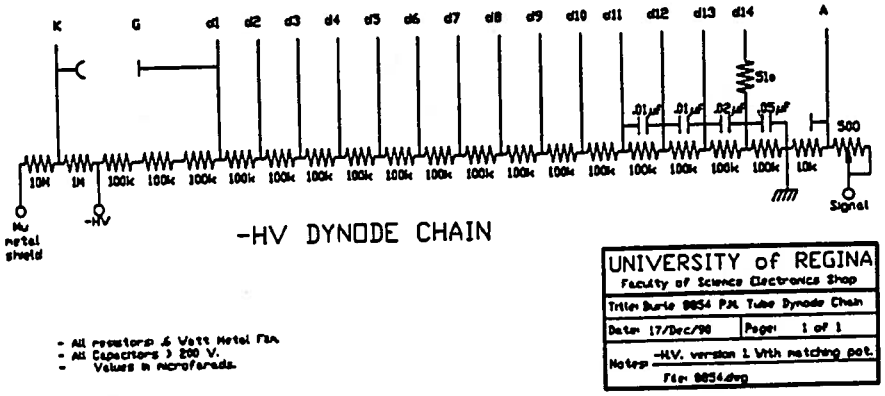

Figure 2: Original Wiring Schematic for Base[2]

2 Description of BURLE 8854 Photomultiplier

2.1 Technical Information

The BURLE 8854 is a 5" photomultiplier. The phototube contains fourteen dynodes. The first of these dynodes has a secondary emitting surface of Gallium-Phosphide (GaP), while the other thirteen dynode surfaces are Beryllium-oxide (BeO). Technical information for the BURLE 8854 appears in Figure 1. The anode performance data listed is from a phototube tested at 2000 V, with a base wiring schematic as in Figure 2.

[1] *BURLE Photomultipliers*, Company Catalog, pp. 26-27

[2] "Manual and Safety Report for CEBAF - Hall A Aerogel Cherenkov Detectors," G. Lolos.

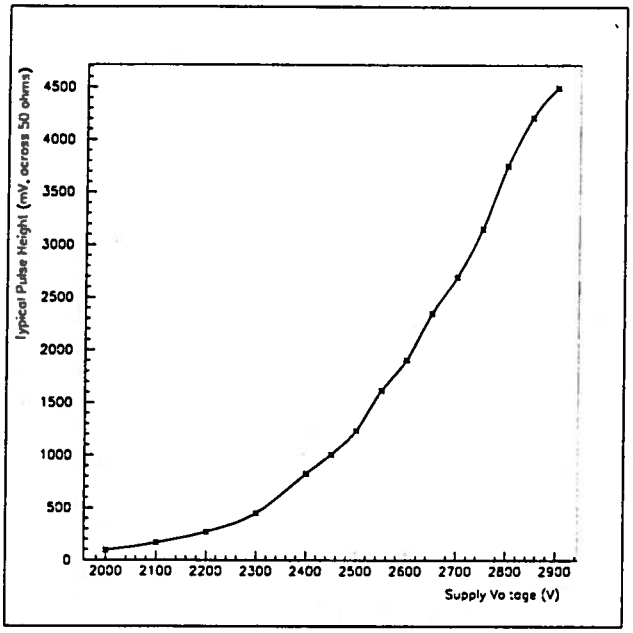

Figure 3: Typical Pulse Height, Base as in Fig. 2 (N90866)

2.2 Original Base Design

The original wiring schematic for the phototube base is shown in Figure 2. It is also important to note that several different phototubes were used throughout this investigation; therefore, there may be differences in values for certain charge measurements from plot to plot. This difference is due to differences in the gain of the individual phototubes. For all of the plots involving data from a phototube, that phototube's serial number has been listed in the caption of the plot in parenthesis.

2.3 Description of Typical Pulse Height and Charge Spectrum

A measurement of the typical pulse height versus supply voltage for the phototube was conducted. The apparatus described in Section 3.1 was used, and the pulse heights were measured directly off of an oscilloscope. The wiring schematic for the base used during these measurements is shown in Figure 2. It was concluded from spectral analysis that these pulse heights were for a single photoelectron. The plot of typical pulse height versus supply voltage is shown in Figure 3.

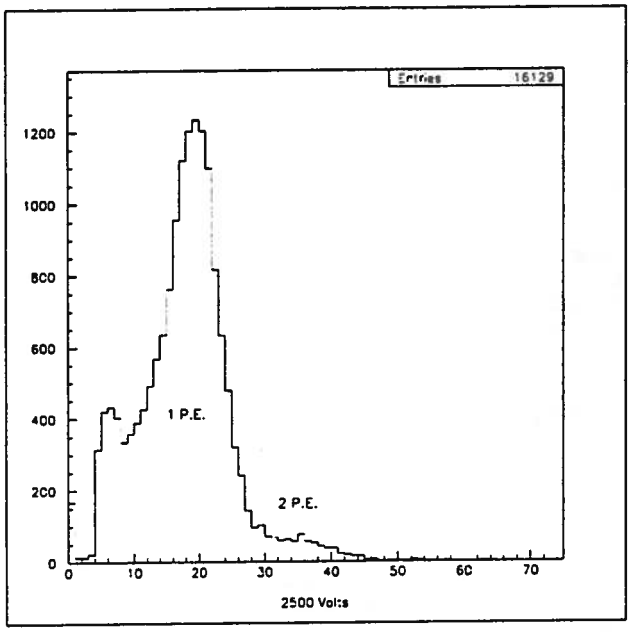

Figure 4: Sample Charge Spectrum, LED on (Z40347)

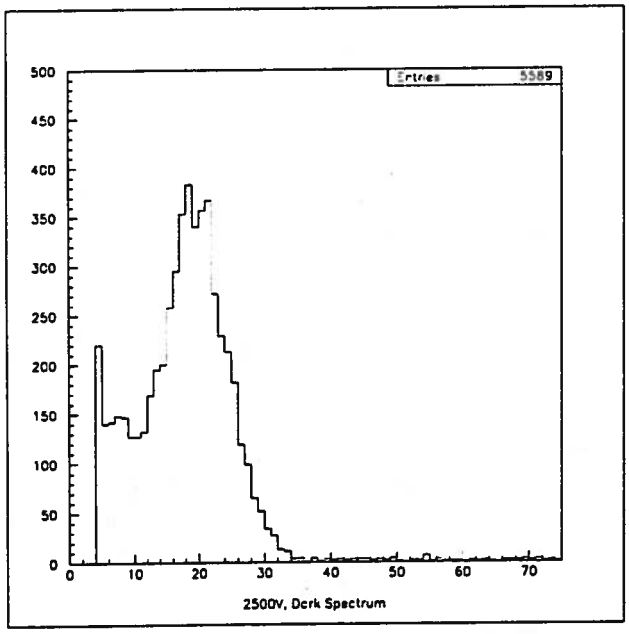

Figure 5: Dark Spectrum, LED off (Z40347)

Second, a brief investigation of the typical charge spectrum of the phototube was conducted. Again the apparatus described in Section 3.1 was used. A sample charge spectrum is shown in Figure 4. The large peak in the charge spectrum is from the pulses which result from a single photoelectron being ejected from the photocathode by an incident photon. A second small peak is visible after the single photoelectron peak which is due to a very small fraction of the events associated with two photoelectrons originating from the photocathode. The most interesting part of the spectrum is what falls just before the single photoelectron peak. It is important to note that these low charge events are not background noise. A second spectrum is shown in Figure 5, this is the spectrum of dark noise which was obtained by using the function generator to gate the ADC and unplugging the LED, instead of creating a gate on a coincidence between the function generator and the PMT. The rate of these background events which were in coincidence with the function generator was up to 50 Hz, which is insignificant compared to the 16 kHz coincidence rate observed when the LED was plugged in. This proved the fact that these low charge events were not merely background noise, but actually caused by the ejection of a photoelectron from the photocathode as a result of an incoming photon from the LED. The phototube was tested with a black shield over the center of the tube leaving only a $1 - 1\frac{1}{2}$" ring of photocathode exposed to the LED light. The spectrum, including the low charge events, appeared the same; thus, conversion from photon to photoelectron on the first dynode is not a possible mechanism for the low charge events. It has been concluded that these events are produced when the original photoelectron elastically collides with the first dynode[3]. In this case no additional electrons are produced at the first dynode. The initial electron just rebounds off the dynode with nearly the same energy, and it continues on the the second dynode where it may interact and produce multiple electrons. Thus a low charge tail is evident below the single photoelectron Gaussian distribution in the total charge spectrum. The relative height of this low charge portion of the spectrum appears to only decrease slightly with increased voltage. The plot in Figure 6 shows the ratio of the average height of the tail to the height of the single photoelectron Gaussian distribution. This tail has important consequences in efficiency analysis and the measurement of the average number of photoelectrons.

[3] *Photomultiplier Tubes, Principles and Applications*, Philips Photonics, pg. 2-9

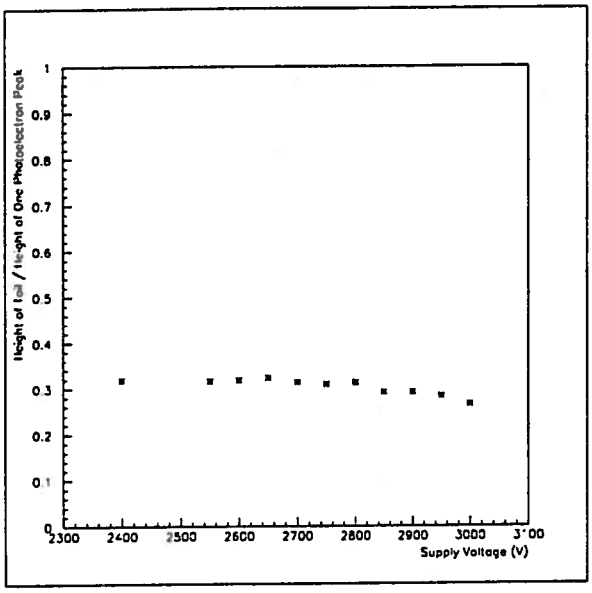

Figure 6: Ratio of tail height to single photoelectron Gaussian height versus voltage; base wiring schematic as in Figure 13 (Z40347)

3 Efficiency

3.1 Apparatus

3.1.1 Production of Photons in Dark Enclosure

The basic idea behind designing the apparatus to study efficiency was to create a device that was capable of delivering a small fixed number of photons to the phototube in a short pulse (Figure 7). To do this a green LED was placed at one end of a dark tube. At the other end of the tube the photomultipler was mounted. At the center of the enclosure there was available space for light attenuating filters.

To pulse the LED, it was driven with a 100 kHz square wave generated by a function generator. A 56 pF capacitor was inserted in series with the LED so the setup yielded a pulse duration of less than 100 ns which was acceptable for the study. Attenuating filters were inserted into the center of the enclosure to precisely adjust the quantity of light striking the phototube.

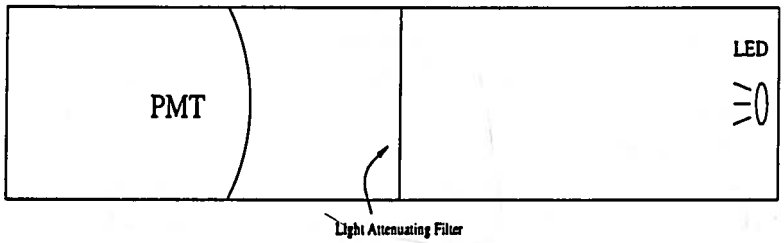

Figure 7: Dark Enclosure with PMT and LED

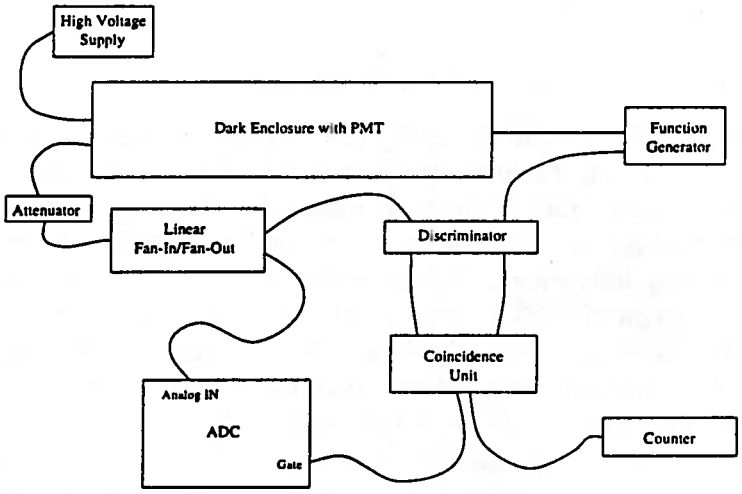

Figure 8: Apparatus for Studying Efficiency

3.1.2 Data Acquisition

The apparatus for studying efficiency appears in Figure 8. The primitive method of measuring efficiency is to advance a scaler counter each time there is a coincidence between the function generator and the phototube. One could then compare the quantity of pulses detected with the quantity of pulses sent. However, it was decided that a more sophisticated method of analysis was necessary. In order to have the ability to view the charge spectrum of the pulses that were being counted, a LeCroy 2249W ADC was installed. The ADC was gated by a coincidence between a phototube pulse and the function generator, and the phototube signal was sent to the analog input for the ADC. An attenuator was also added so the amplitude of the pulses coming from the PMT could be controlled. This was necessary to avoid saturating the Linear Fan-In/Fan-Out. A test of the linearity of this attenuator was conducted and the results are presented in Section 4.1.3. With this apparatus, a detailed study of the efficiency of the phototube could be conducted.

3.2 Results

3.2.1 Fixed Threshold Analysis With Scalar

The most basic method of studying the efficiency of the phototube, as mentioned above, is simply to compare the number of pulses detected by the phototube with the number of pulses sent from the LED. By using the ADC, the minimum voltage at which the single photoelectron peak is above the 10 mV threshold was determined. Voltage was then varied from that minimum up to the maximum of 3000 V. Scalar data for 10 s intervals are shown in the plot in Figure 9. Each event is the result of a pulse in coincidence from both the phototube and the function generator driving the LED. At each voltage, data was taken with the LED unplugged in order to correct the counts for accidental background coincidences. The increase in background counts at the higher voltages is due to the phototube noise triggering the the discriminator with the low 10 mV threshold.

From the plot in Figure 9 one can conclude that there is a definite increase in the number of detected pulses. Analysis of the charge spectrum, described in Section 2.3, concludes that a noticeable portion of the single photoelectron spectrum is below the Gaussian distribution of the single photoelectron peak. It is probable that this apparent increase in efficiency is due to the inclusion of more low charge events. From the plot in Figure 10, it can be seen that at the lowest voltage the threshold is still below the sin-

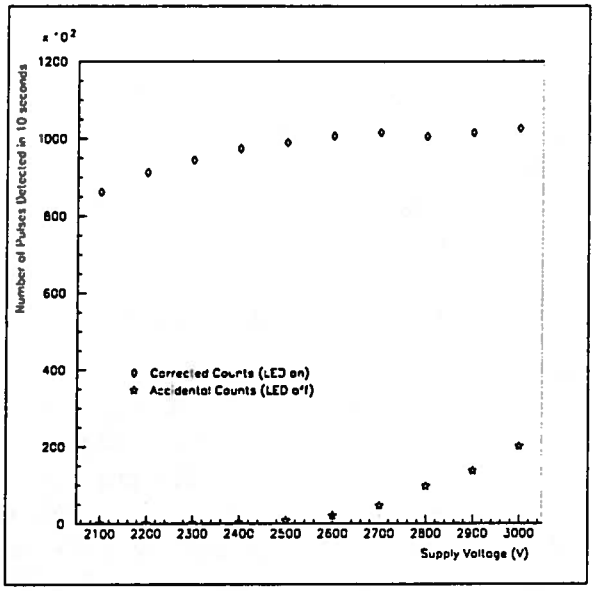

Figure 9: Pulses Detected vs. Supply Voltage (fixed threshold at 10 mV) (N32545)

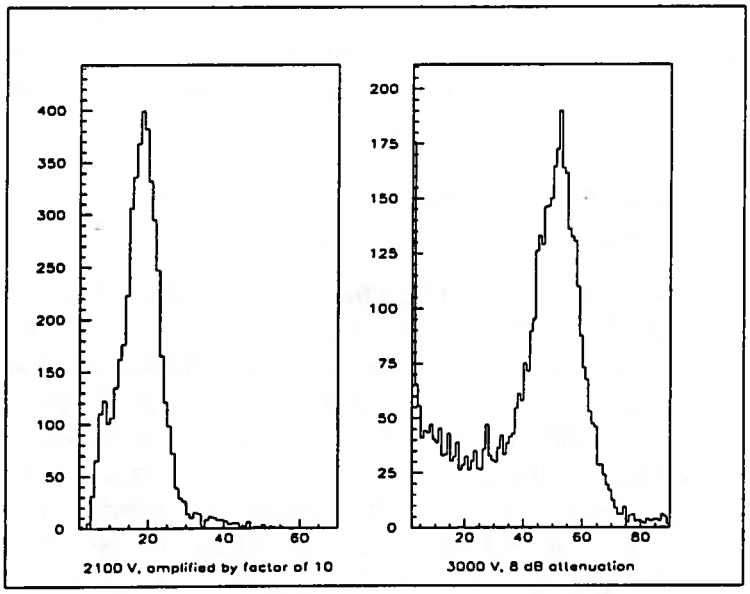

Figure 10: Charge Spectra at 2100 V and 3000 V (10 mV threshold not visible in 3000 V spectrum because of 8 dB attenuation in contrast to amplification factor of 10 in 2500 V spectrum) (N32545)

gle photoelectron amplitude; however, as the voltage is increased this single photoelectron peak and all of the low charge events increase in amplitude. Thus, with the fixed threshold it is possible for one to include the events under the single photoelectron peak each time, but with each increase in voltage include more low charge events.

3.2.2 High Statistics Analysis for Two Different Total Voltages

To better examine the effect of voltage on efficiency, two high statistics runs were taken. For each of these runs, the ADC was gated by the function generator; therefore, every time a pulse was sent to the LED, a gate was sent to the ADC. The spectra appear in Figure 11. The single photoelectron peak was fitted to a Gauss function, and the mean of the peak was determined from the from the fit. The pedestal, created by LED pulses which the phototube did not detect, appears around the first few bins of the histogram, and it was also fitted to a Gauss. The pedestal was then subtracted from the mean to determine the actual mean. The number of events above 30% of the actual mean plus the pedestal were determined and compared for both plots. These tabulations are shown in Figure 12. One can note that when considering events above a fixed relative threshold (based on the single photoelectron peak) there is relatively no difference in efficiency between an operating voltage of 2500 V and 2900 V.

3.2.3 High Statistics Analysis for Two Different Cathode to First Dynode Voltages

It is also necessary to examine the effect of greatly changing the electric field between the photocathode and the first dynode. In order to do this, the resistance in the circuit between the photocathode and the first dynode was doubled (from $300k\Omega$ to $600k\Omega$). Making this change in resistor values produces a change in the field from the photocathode to first dynode that is 4 times larger than the change as a result of only increasing the supply voltage as above (Section 3.2.2). Two voltages were selected, one for the $300k\Omega$ setting and one for the $600k\Omega$ setting. These voltages were selected in such a way that the voltage across the dynode chain remained constant for both, and the field between the photocathode and the first dynode was doubled. The data, which appear in Figure 14, were analyzed in the same manner that the two previous runs were analyzed (Section 3.2.2). The numbers of counts above 30% of the adjusted mean of the distribution were compared. However, this time a small increase in the number of counts was

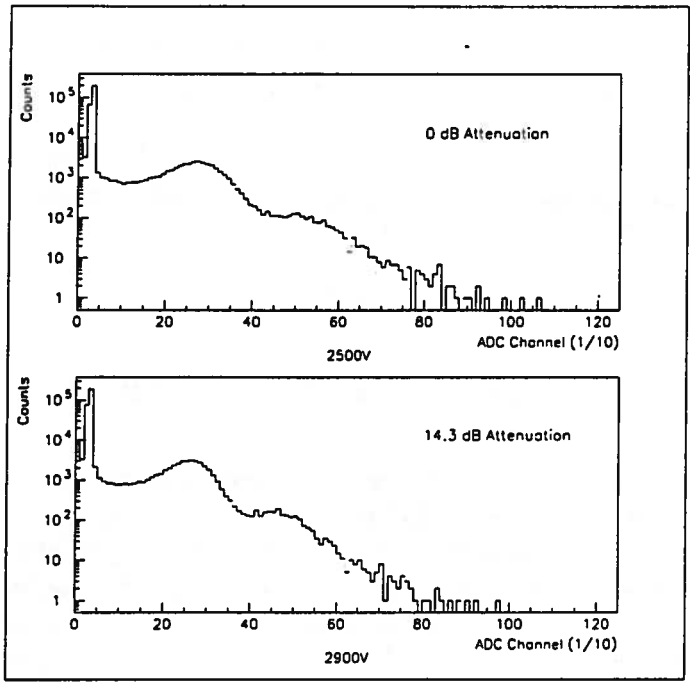

Figure 11: High Statistics Runs at 2500 V and 2900 V (Z40347)

2500V 0dB

Mean of 1PE=25.9
Pedestal =3.19

Actual Mean=22.7

30% of Actual Mean=6.8
Add Pedestal +3.2

Determine Events Above channel 10.0

44,210

2900V 14.3dB

Mean of 1PE=26.9
Pedestal =3.21

Actual Mean=23.7

30% of Actual Mean=7.1
Add Pedestal +3.2

Determine Events Above Channel 10.3

Above 10- 43,320
Above 11- 42,540

Above 10.3=(.7)(N10-N11) + N11

43,820

Decrease of events by 0.88% +- 0.67%

Figure 12: Tabulations for High Statistics Runs

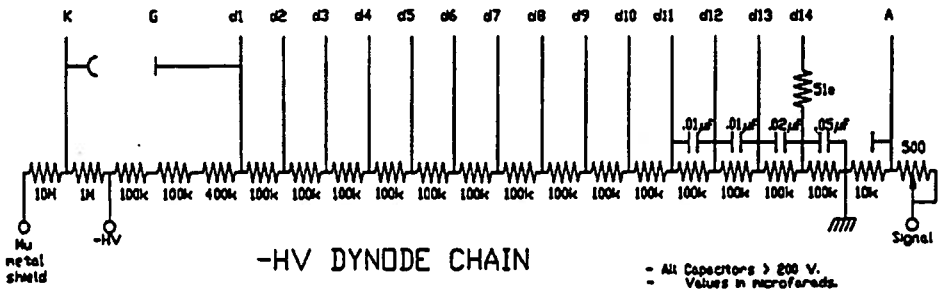

Figure 13: Wiring Schematic for Base With $600k\Omega$ Resistance

noticed. One can speculate that this small increase in counts above the fixed relative threshold is due to the fact that as the field between the photocathode and the first dynode is dramatically increased, the probability that the photoelectron will elastically rebound off of the first dynode is decreased; therefore, more pulses are likely to fall under the single photoelectron Gaussian distribution than in the tail below the Gaussian. The tabulations for the data are shown in Figure 15. Another effect of this increase in resistance between the cathode and dynode is a slight decrease in the overall gain of the phototube.

3.3 Efficiency Analysis Using Actual Cherenkov Radiation

Previous analysis of efficiency was performed with a green LED. The LED apparatus was preferred because it was easy to control the parameters of the testing with such an apparatus. However, it was necessary to test the phototube also with Cherenkov light (which is primarily in the ultra-violet portion of the spectrum). In order to conduct this analysis modifications to both the photon source and the data acquisition system were necessary.

3.3.1 Apparatus Modifications

The apparatus for delivering Cherenkov radiation to the phototube is pictured in Figure 16. The Cherenkov light is emitted when an electron from the beta emitting source Strontium-90 passes through the quartz radiator mounted on the front of the source. This Cherenkov light is then reflected off of a series of two mirrors made from aluminized-mylar (the aluminum is used as the reflecting surface) back to the phototube under test. The photocathode window limits the transmission of Cherenkov radiation. Lower

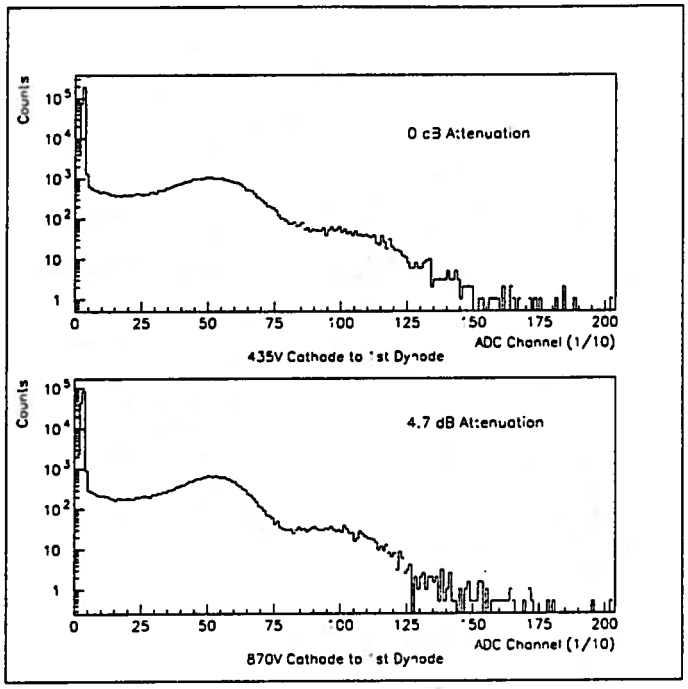

Figure 14: High Statistics Runs at Different Cathode to 1st Dynode Voltages (Z40347)

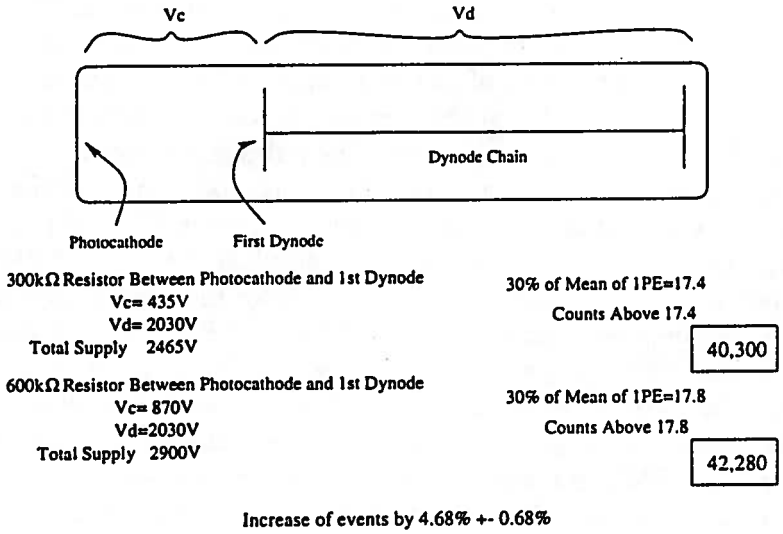

Figure 15: Tabulations for High Statistics Runs

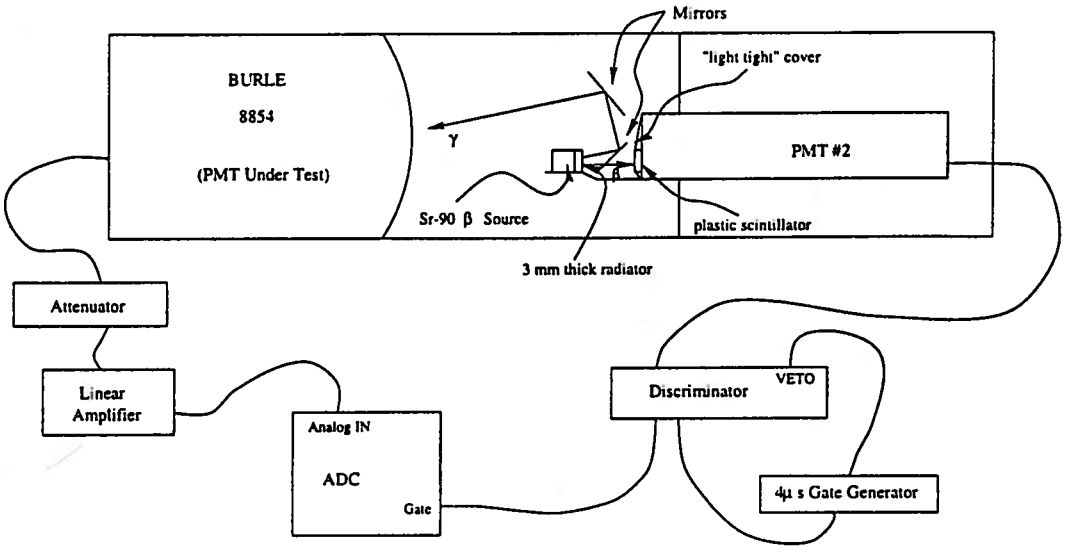

Figure 16: Apparatus for Delivering Cherenkov Radiation to Phototube

energy beta particles also enhance the ultra violet portion of the spectrum. Thus it can be concluded that the spectrum of Cherenkov light used for this analysis is nearly identical to the spectrum received by the phototube in the actual gas Cherenkov detector. The electron which produced the Cherenkov radiation continues through the first mirror and strikes a plastic scintillator which is sealed from the rest of the apparatus. The luminescence of the scintillator produces a pulse in the second phototube which is used as a trigger for the data acquisition system. The pulse generated in the phototube being tested can then be sent directly to the analog input of the ADC. The discriminator was shut off for $4\mu s$ after a pulse in PMT #2 to avoid triggering the data acquisition system on afterpulses. The rate of PMT #2 was around 45 Hz. With the source removed from the apparatus, the rate only measured between 1 Hz and 2 Hz. The rate of PMT #2 was carefully monitored throughout the experiment. Any significant decay background noise would increase the fraction of events detected by the phototube under test. This would then appear as a false increase of efficiency in the results. For this reason, PMT #2 was powered up 6 - 8 hours before data taking began, and a voltage of 1400 V was maintained on the phototube until all of the runs were finished.

	Increase in Efficiency	Error
Full Photocathode	4.5%	0.5%
Outside Edge Only	4.2%	1.0%
Center Only	5.6%	1.1%

Figure 17: Results of tests performed with Cherenkov radiation; total supply voltage was increased from 2500 V to 2900 V, base wiring schematic as in Figure 13 (N32545)

3.3.2 Results

The same technique that was used in for previous high statistics efficiency analysis (Sections 3.2.2 and 3.2.3) was used for the analysis of this data. The numbers of events above 30% of the mean were compared. With the green LED efficiency was not noticeably effected by increasing the supply voltage from 2500V to 2900V. However, when the Cherenkov light was used for the testing, there appeared to be a slight increase in efficiency with the same increase in supply voltage. The results of these tests with Cherenkov radiation are shown in the table in Figure 17. In order to see if the efficiency change was dependent on where the incident light strikes the photocathode, the phototube was tested with only a $\frac{3}{4}$" ring around the edge of the photocathode exposed to the light source. It was also tested with just a $2\frac{1}{2}$" circle in the center of the photocathode exposed. For these tests, black tedlar was used to shield portions of the photocathode from the incident light. The rest of the apparatus remained unchanged. From the results in Figure 17, it can be concluded that increasing the supply voltage to the phototube from 2500 V to 2900 V increases the efficiency at which the phototube detects Cherenkov radiation by 4 to 5 percent. This increase does not appear to strongly depend on where the incident photon strikes the photocathode.

4 Saturation

4.1 Apparatus

4.1.1 Modification of Photon Source

It was necessary to modify the apparatus in order to investigate the linearity of the phototube (Figure 18). In order to saturate the phototube, or produce more charge than the base in conjunction with the phototube could handle in a short amount of time, multiple photons had to be delivered to the

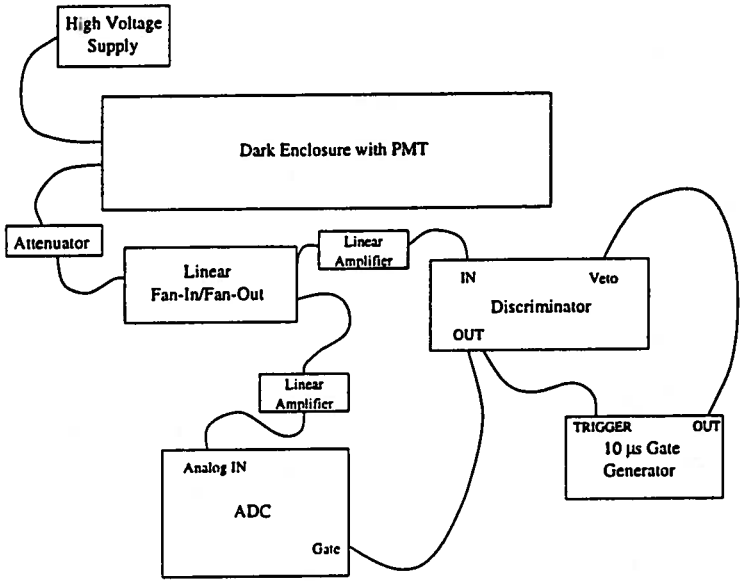

Figure 18: Apparatus for Studying Saturation

phototube simultaneously. The LED setup was not capable of achieving this. Therefore, it was replaced with a radioactive source and a piece of plastic scintillator. The alpha particle emitting source Americium-241 was used to make the scintillator luminesce. With the alpha source and scintillator it was possible to generate short pulses of multiple photons. The defined peak around bin 100 in the spectrum in Figure 20 demonstrates the ability of the alpha source to produce roughly the same number of photons with each pulse. These pulses could then be passed through the light attenuating filter if necessary.

4.1.2 Modification of Data Acquisition System

Modifications to the data acquisition system were also necessary. If large pulses are generated by the phototube, occasionally afterpulses are also generated. An afterpulse is a pulse caused by ionization of molecules of gas inside of the dynode chamber which may interact with the dynodes creating a pulse which was not a direct result of an incident photon. Such afterpulses should not be included in the analysis. The pulse rate of the source was estimated to be around 10 kHz. Immediately after the large initial pulse, a $10\mu s$ pulse was sent to the discriminator to keep it from triggering on any of the afterpulses. This helped to remove afterpulses from the charge spec-

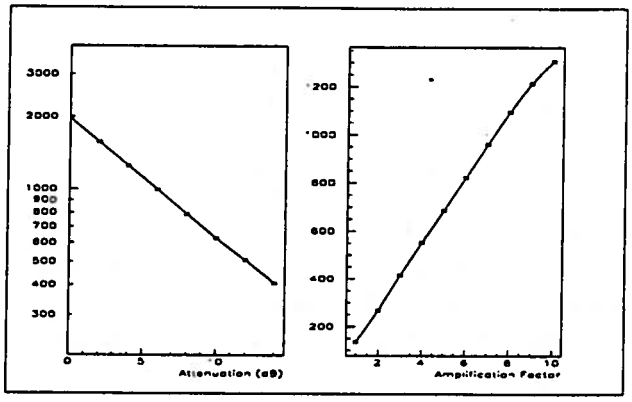

Figure 19: ADC Channel vs. Amplifier and Attenuation Settings

trum of the recorded pulses. The gate for the ADC was the discriminated phototube signal. The width of this gate was set to approximately 80 ns to include the initial pulse and avoid including any afterpulsing.

4.1.3 Testing of Associated Linear Amplifiers and Attenuators

Linear amplifiers were also added after the Linear Fan-In/Fan-Out in order to deal with small pulses. The linearity of both the attenuator and the amplifier were tested by passing a 500 mV square pulse through them and viewing the ADC spectra for different amplifications and attenuations. The attenuator appeared to perform linearly and the amplifier was linear up to around 4 V. The plots for these tests are shown in Figure 19.

4.2 Theory

In theory, a plot of the log of the gain versus the supply voltage should be linear. Linearity of this plot is important in the analysis of the data, because if one knows that the phototube performs linearly the number of photoelectrons produced at the photocathode can be easily determined. This can be shown in the following manner. Let the total gain of the photomultiplier be equal to M, and M_i be the gain on each dynode of a phototube with n dynodes.

$$M = \prod_{i=1}^{n} M_i \tag{1}$$

Assume that the gain on each dynode is roughly the same (M_1). Thus the log of the total gain can be expressed in the following way from Equation 1.

$$log(M) = n(log(M_1)) \tag{2}$$

Where M_1 is the average gain of the dynodes. One can now approximate an equation that would relate the gain on one of the dynodes with the potential difference between that dynode and the previous one. Let $f(V)$ be the gain as a function of this potential difference, or voltage. Assuming this function can be approximated by the first two terms of a Taylor expansion, the gain on a single dynode can be written in the following manner.

$$M_i = f(V_o + \Delta V) = f(V_o) + f'(V_o)\Delta V \tag{3}$$

Where $f(V_o)$ is the gain at some initial voltage. Substituting Equation 3 into Equation 2 and simplifying will yield the follow equation.

$$log(M) = n\left(log\left(f(V_o)\right) + \frac{f'(V_o)}{f(V_o)}\Delta V\right) \tag{4}$$

From Equation 4 one can note that the relationship between $log(M)$ and ΔV is linear. However, as soon the phototube is not able to produce high amounts of charge, this plot will deviate from linearity and approach a maximum value. The point at which this deviation from linearity occurs is determined by how the phototube base is designed.

4.3 Results

4.3.1 Method of Analysis

The linearity of the phototube was tested with the apparatus described in Figure 18. Kodak photographic filters were used as light attenuating filters. The source of light, as described above, was a plastic scintillator which was activated with an alpha source. Data was taken for a variety of voltages with light being attenuated by 0%, 68%, and 90% (corresponds to the plots of 100%, 32%, and 10% emission in Figure 21 and Figure 23). A large contribution to the single photoelectron peak as a result of background noise was noticed. Figure 20 shows a sample charge spectrum from the saturation study. The characteristic pulse charge is determined by fitting the broad peak around bin 100 to a Gauss function. By using spectra at low voltages and assuming linearity the average number of photoelectrons per pulse at 100% emission was estimated to be around 30.

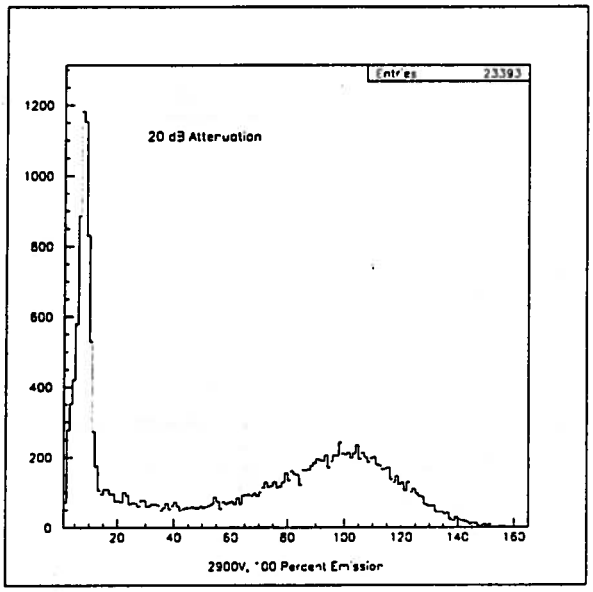

Figure 20: Sample Charge Spectrum from Apparatus for Studying Saturation (N32545)

4.3.2 Performance of Original Base

The phototube base with the $600k\Omega$ cathode to first dynode resistance (shown in Figure 13) was tested in the manner described above. The plot in Figure 21 shows how the tube begins to saturated around 700 pC. The single photoelectron points were extracted from the plots by fitting the sharp single photoelectron peak (shown in Figure 20 around bin 8). The tube appears to be linear along the single photoelectron points and the set of points for 10% emission ($\approx$ 3 photoelectrons). Deviation from linearity is definitely evident in both the 32% and 100% emission curves. This deviation from linearity is due to space charge effects of large amounts of electrons being produced around the last dynodes during the creation of a pulse. This large number of electrons disrupts the electric field between the last few dynodes causing a reduction in the gain of the final dynodes, which is characterized by the saturation seen in Figure 21. If there was a correlation between a position on the photocathode and a position on the anode, it is possible for this space charge effect to be enhanced in such a way that it would make the phototube saturate at a lower charge. If a large burst of photons hit the photocathode in one particular spot, all of the secondary electrons would be focused to one particular spot of the anode making the space charge effect

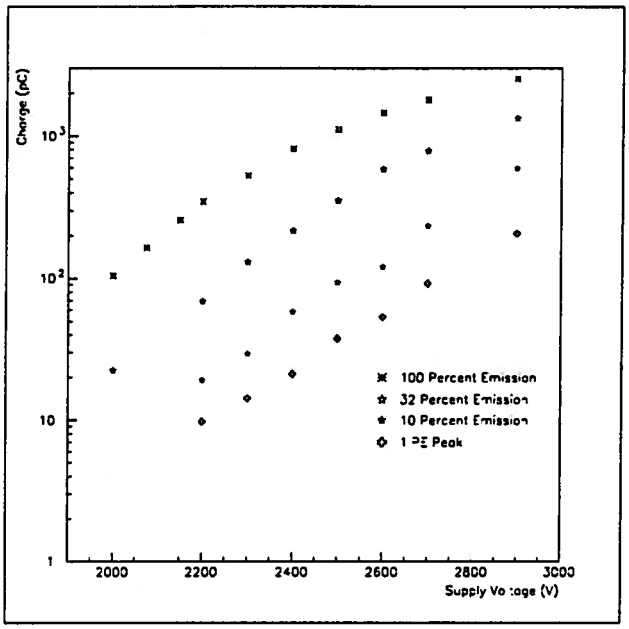

Figure 21: Saturation Curve for Base in Figure 13 (N32545)

considerably larger in that local area of the anode. In order to avoid this deviation from linearity, or saturation, modification of the phototube base was necessary.

4.3.3 Performance of Modified Base

A popular method to counteract the effects of space charge is to make the electric field progressively larger between the last few dynodes. By doing this, the effect of the space charge is much less significant. This progressive increase in electric field can be made by increasing the value of the resistors between the last few dynodes. The base was modified in this manner and the wiring schematic for the modified base is shown in Figure 22.

This modified base was tested using the same procedure as described above. The results of this test are shown in Figure 23. A few things can be noted from this plot. First, all of the plots of charge versus voltage are linear. This would suggest that the saturation problem has been solved. From the plot one can conclude that the phototube performs linearly at least up to a charge of nearly 3000 pC. This is an improvement on the 700 pC saturation point of the original base. The second thing to notice from this plot is that this increase in the linearity of the comes at an expense of gain. The gain

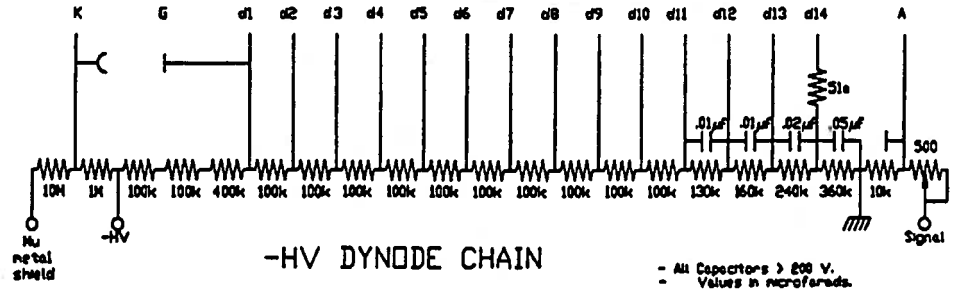

Figure 22: Wiring Schematic for Base With Modified Resistor Values

of the phototube appears to decrease by a factor of 5 (from the comparison of Figure 21 and Figure 23). This decrease in gain is due to the fact that the total current through the resistive divider is decreased, thus decreasing the voltage between all of the dynodes for which the resistor value was not changed. Actual data from the Hall A Gas Cherenkov detector at TJNAF is shown in Figure 24. At the top of the figure is the spectrum produced with the original base design. The spectrum at the bottom was produced with the same phototube and a modified base.

4.3.4 Resistive Divider Current and Mean Anode Current

One must make sure that the current through the resistive divider is always significantly large compared to the mean anode current. This comparison can be examined for the modified base (Figure 22). Consider the values for 100% emission at 3000 V. At this point the anode charge per pulse is around 3 nC (from Figure 23). The rate of the pulses from the radioactive source is around 10 kHz. Thus the mean anode current can be calculated in the following manner. Let I_a equal the mean anode current.

$$I_a = \left(3 \times 10^{-9} C\right)\left(1 \times 10^4 \frac{pulses}{second}\right) = 30\mu A \tag{5}$$

The current through the resistive divider (I_d) can then be calculated using the total resistance of the divider and the applied voltage. For the case being considered these values are $2.5M\Omega$ and 3000 V respectively.

$$I_d = \frac{3000V}{2.5M\Omega} = 1.2mA \tag{6}$$

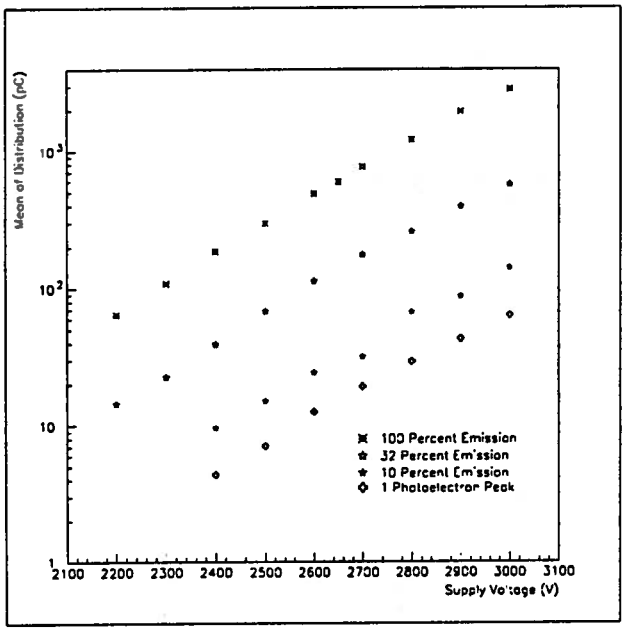

Figure 23: Saturation Curve for Base in Figure 22 (N32545)

From Equations 5 and 6 and Figure 23 it can be concluded that the base appears to perform linearly at least to pulse charges of around 3000 pC while the ratio of the anode current to divider $\left(\frac{I_a}{I_d}\right)$ remains under 0.025.

5 Effect of 500Ω Variable Resistor at Anode

The effect of the 500Ω variable resistor at the anode (shown in Figures 2 and 13) on pulse size was also examined. To do this the mean of the single photoelectron distribution was measured. The tube was operated at 2500 V and the resistor setting was varied from 0Ω to 500Ω. The results are shown in Figure 25. As expected there was a very slight decrease (< 6%) in the mean pulse charge as the resistor was varied through its full range. This slight decrease is due to the fact that as the resistor is increased more of the charge is routed through the $10k\Omega$ resistor (also shown in all of the base wiring schematics) to ground.

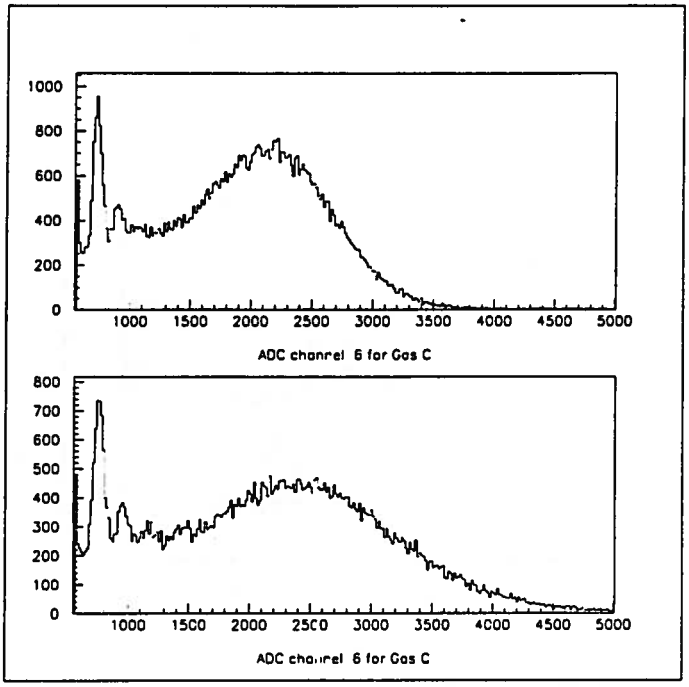

Figure 24: Actual Gas Cherenkov Data, top spectrum with original base and bottom spectrum with modified base, both taken with the same phototube (0.1 pC/Channel)

Resistor Setting (Ω)	Mean of Distribution (pC)
0	328.0
98	324.5
199	316.5
304	313.8
404	311.3
501	309

Figure 25: Mean of Distribution vs. Anode Variable Resistor Settings (N90866)

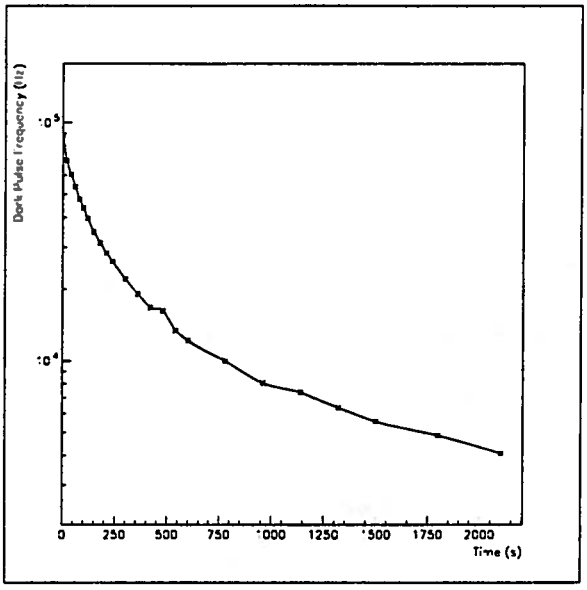

Figure 26: Decay of Dark Noise After Exposure to Light for 100 s (Z40347)

6 Decay of Dark Noise

In order to study the decay of dark noise the photocathode was exposed for a period of 100 seconds in a brightly lit room. The tube setup was then reinserted into the dark enclosure, and a voltage of 2900 V was applied to the tube (the wiring schematic for the base during this testing is shown in Figure 13). The phototube signal was passed through a discriminator with a 20 mV threshold. Immediately after the application of voltage, scaler counts were taken at regular intervals. The plot of the dark pulse frequency versus time appears in Figure 26. The plot in Figure 26 is for one particular phototube. Other phototubes were tested and the plots were of similar shape.

7 Monte Carlo Simulation

7.1 Goal

The goal for the Monte Carlo simulation was to create a tool to study different aspects of the charge distribution from the photomultiplier tube. The simulation provided a means to study parameters that could not be easily controlled in a real experiment. This allowed different aspects of the genera-

tion of the spectrum to be studied separately. The most important result of the study of the Monte Carlo simulation was a quantitative understanding of the relationship between the charge spectrum of the photomultiplier tube and the average number of photoelectrons ejected from the photocathode.

7.2 Creating the Simulation

The program was modeled after real data collected from the Burle 8854 phototube (serial number Z40347, base configuration as seen in Figure 13). Modifications were made to the program to allow it to simulate different 8854 tubes with slightly different gains. Data taken in actual experiments were used to model the variation of the mean and standard deviation of the single photoelectron peak as voltage is varied. The mean of the single photoelectron peak (not including the tail on the front of the spectrum) was found to fit the following relationship:

$$A = (2.5pC)Exp\left(\frac{V - 1702}{264}\right) \tag{7}$$

Where A is the mean of the single photoelectron peak, and V is the voltage supplied to the phototube. The standard deviation of the single photoelectron peak (again, disregarding the tail on the front of the distribution) was found to be modeled by the following relationship:

$$\sigma = (2.5pC)Exp\left(\frac{V - 2074}{294}\right) \tag{8}$$

Where σ is the standard deviation of the single photoelectron peak, and V is the voltage supplied to the phototube. The relationships were normalized to be the same as the output of the ADC rebinned by a factor of 10. Conversion from bins to a charge scale requires a multiplication by 2.5 pC/Bin. The distribution for the single photoelectron peak was simulated by a Gaussian shape and a tail that represents an even distribution of events lower in charge than the mean (whenever the value of the Gaussian is less than a constant, that constant is used to represent the height of the tail). This added tail changes the mean and standard deviation of the entire distribution according to the statistical definitions. The Gaussian shape used to model the single photoelectron peak (without the tail) is given by:

$$P(x, A, \sigma) = e^{-\left(\frac{(x-A)^2}{2\sigma^2}\right)} \tag{9}$$

The mean of the Gaussian is given by A, the standard deviation is given by σ, and the desired position for which the relative probability is to be found

is given by x. This Gaussian always has a maximum height of one. The tail on the front of the Gaussian has a nearly constant height relative to the height of the Gaussian peak over the range of the experimental data. A slight correction was added for larger values of the mean of the single photoelectron peak, where the relative height of the tail decreases. The distribution of initial photoelectrons was assumed to follow a Poisson distribution given by:

$$P(n,\mu) = \frac{\mu^n e^{-\mu}}{n!} \tag{10}$$

The mean of the Poisson, the mean number of photoelectrons emitted from the photocathode, is given by μ, and n is the value for which the probability is being calculated.

Fitting the data to functions allowed new points to be interpolated (and extrapolated if necessary). Charge spectra for multiple photoelectrons ejected from the photocathode were simulated by summing the charge from separate one photoelectron events. This algorithm is accurate as long as there are no saturation effects. A sample spectrum produced by the Monte Carlo simulation can be seen in Figures 27 and 28. The spectrum in Figure 28 simulates four initial photoelectrons, but it is already noticeably shifted toward lower charge. One of the main purposes of the Monte Carlo simulation was to investigate unexpected properties of the charge spectra due to the additional low charge events included in the single photoelectron spectrum.

The Monte Carlo simulation produces not only the complete charge spectrum from a phototube, but also the spectra of individual numbers of initial photoelectrons. This way the individual Gaussians that make up the spectra for larger numbers of photoelectrons can be individually analyzed. An example of this can be seen in Figure 29. This feature was used to check that the mean of each individual distribution was located at an integer multiple of the mean of the single photoelectron distribution. The mean (calculated from the statistical definition) of the entire distribution was also checked against the distribution of the single photoelectron peak, and the ratio was found to accurately describe the number of photoelectrons.

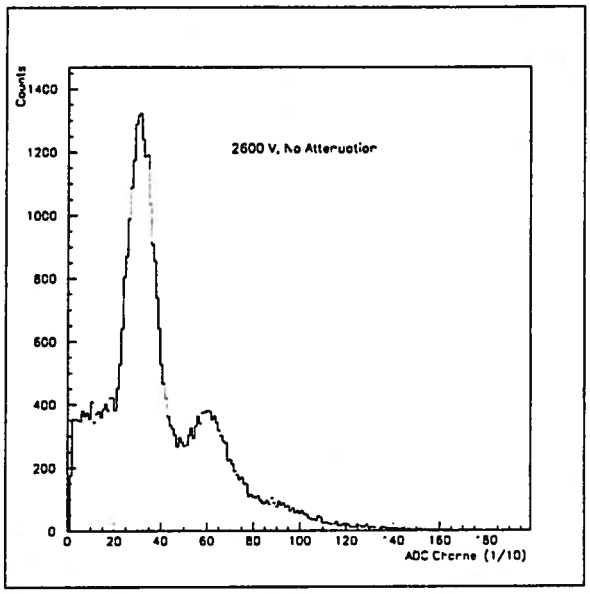

Figure 27: Monte Carlo Simulation with One Photoelectron Average

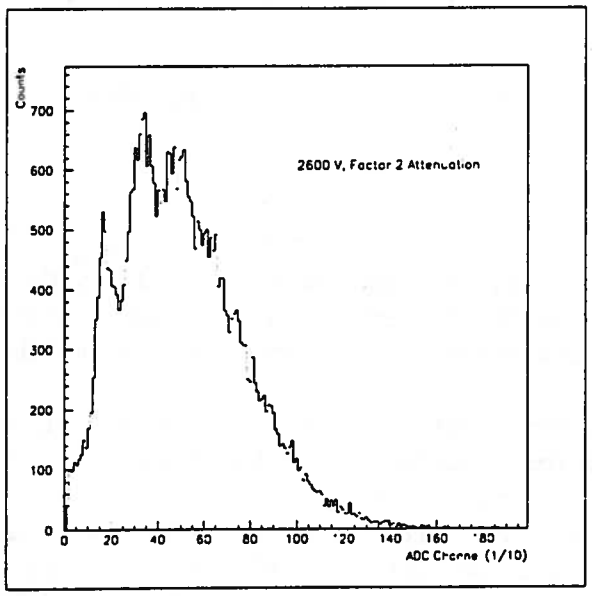

Figure 28: Monte Carlo Simulation with Four Photoelectrons Average

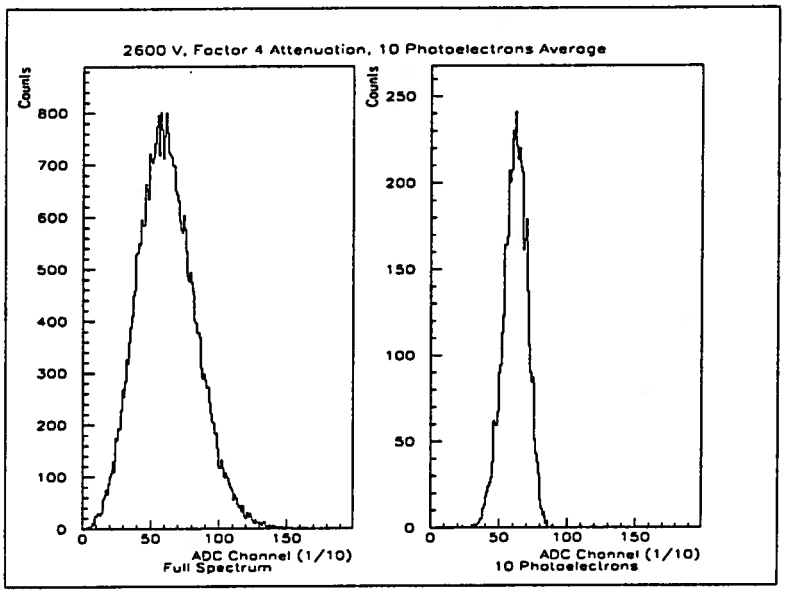

Figure 29: Separation of Complete Spectrum into Constituent Spectra

7.3 Analyzing the Number of Photoelectrons

The simulation was created to find a relationship between the charge spectra and the average number of photoelectrons. An often used relationship is given by:

$$N = \left(\frac{A}{\sigma}\right)^2 \tag{11}$$

The mean of the entire distribution is given by A, the standard deviation of the entire distribution is given by σ, and the average number of photoelectrons is given by N. This result can be derived from the Poisson distribution.

In order to insure correctness in finding the average number of photoelectrons, the simulation was run with different functions for the single photoelectron peak to check the code. A relationship between the spectra and the number of photoelectrons was found. The applicability of Equation 11 to the various spectra was studied, as well as any adjustments to the formula necessary to account for differences in the model for the single photoelectron peak. Simulations were run with averages of ten and fifteen initial photoelectrons, the range most important for the gas Cherenkov counter.

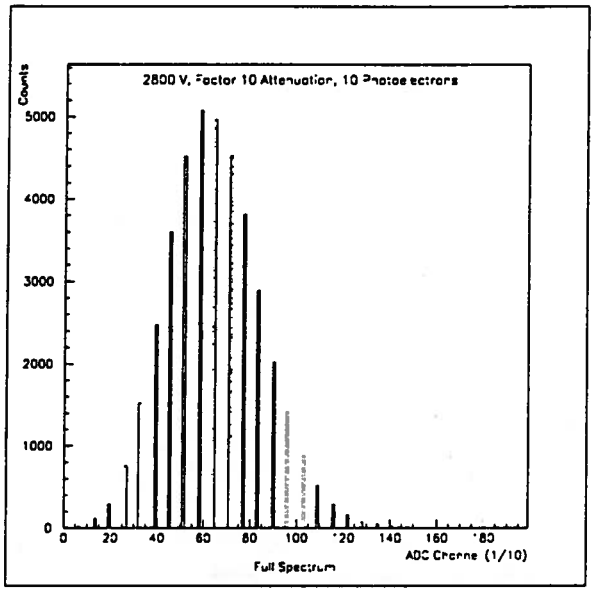

Figure 30: Poisson Distribution without Gaussian

7.3.1 Poisson Distribution without Gaussian

The first test was to analyze the Poisson distribution using only a constant for the single photoelectron spectrum. The full distribution was then a perfect Poisson. The resulting spectrum was analyzed both by calculating the mean and standard deviation from the statistical definitions and by Gaussian fitting as would be the most likely method of analysis of real data. An example of this type of spectrum is shown in Figure 30. The mean and standard deviations found by the statistical definitions fit Equation 11 very well, as was expected.

7.3.2 Poisson Distribution with Gaussian

Consider the single photoelectron peak as modeled by a perfect Gaussian. Multiple photoelectron peaks are built as sums of single photoelectron events. When all of these Gaussians are summed together, the standard deviation of each Gaussian contributes to increasing the standard deviation of the resulting distribution. The standard deviation of the resulting distribution (calculated from the statistical definition) is greater than the standard deviation of the Poisson distribution. This explains the fact that the number of photoelectrons predicted by Equation 11 using data from this type of distri-

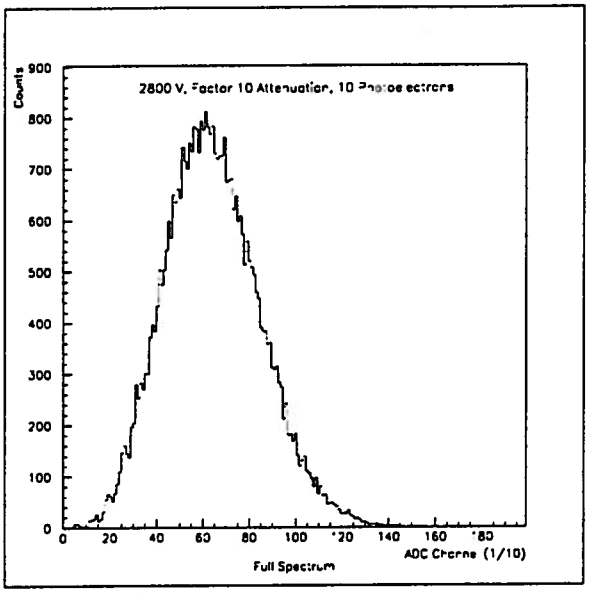

Figure 31: Poisson Distribution with Gaussian

bution is smaller than if the distribution was simply a Poisson. An example of this spectrum is shown in Figure 31.

7.3.3 Poisson Distribution with Model for Actual Distribution

The low charge events on the leading edge of the single photoelectron Gaussian have a great effect on the full spectrum. This tail increases the standard deviation of the full spectrum and decreases the mean of the single photoelectron distribution in the following way:

$$A_{Distribution} = 0.80 A_{Peak} \tag{12}$$

The mean of the entire single photoelectron distribution is $A_{Distribution}$ and A_{Peak} represents the mean of the single photoelectron peak (as if the peak was Gaussian - disregarding the tail). The effects of this tail account for the fact that using the mean and standard deviation of this spectrum (from statistical definitions) in Equation 11 results in a lower number of predicted photoelectrons than if the distribution was simply Poisson. The change in the number of photoelectrons calculated using Equation 11 is larger for this model of the single photoelectron spectrum than for the model using only a Gaussian shape. Figure 32 shows an example of this kind of spectrum.

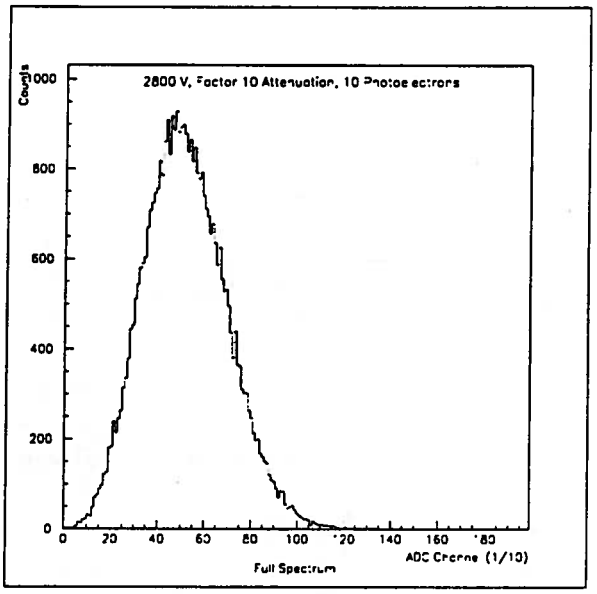

Figure 32: Poisson Distribution with Model for Actual Distribution

7.3.4 Data

The contributions of each of these effects was studied by modifying the Monte Carlo program and studying the resulting histograms by calculating the actual mean and standard deviation (according to the statistical definition) and also by analyzing the data in PAW. A summary of this information can be see in the table in Figure 33. The column *Photoelectrons* is the average number of initial photoelectrons. The column *Function* describes what kind of function the Monte Carlo was using to describe the single photoelectron distribution. *No Gauss* indicates that mean of the single photoelectron distribution was substituted for the Gaussian distribution, so the resulting spectrum is discrete. *Gauss w/o Tail* indicates that the single photoelectron peak was modeled as a perfect gauss without the tail on the front of the distribution. Finally, *Gauss with Tail* indicates that the simulation was run with the spectrum fit from actual data - a Gaussian with a tail on the leading slope (less than the mean). The column *Method* indicates whether the analysis was done with the statistical definitions of mean and standard deviation or with a Gaussian fit of the spectrum. The column $(A/\sigma)^2$ lists the values calculated using Equation 11.

Photoelectrons	Voltage (V)	Function	Method	$(A/\sigma)^2$
10	2800	No Gauss	Statistics	10.04
			Gauss Fit	7.92
		Gauss w/o Tail	Statistics	9.63
			Gauss Fit	7.42
		Gauss with Tail	Statistics	8.28
			Gauss Fit	5.62
	2400	No Gauss	Statistics	10.07
			Gauss Fit	7.64
		Gauss w/o Tail	Statistics	9.54
			Gauss Fit	7.00
		Gauss with tail	Statistics	8.47
			Gauss Fit	6.21
15	2800	No Gauss	Statistics	14.99
			Gauss Fit	11.55
		Gauss w/o Tail	Statistics	14.78
			Gauss Fit	11.63
		Gauss with Tail	Statistics	12.52
			Gauss Fit	9.44
	2400	No Gauss	Statistics	15.01
			Gauss Fit	11.23
		Gauss w/o Tail	Statistics	14.50
			Gauss Fit	11.63
		Gauss with tail	Statistics	12.46
			Gauss Fit	9.80

Figure 33: Table of Data for Determining Number of Initial Photoelectrons

7.4 Analysis of Spectra

7.4.1 Method Using the Quantity $\left(\frac{A}{\sigma}\right)^2$

Another effect on the number of photoelectrons calculated by Equation 11 is the way in which values of A and σ are obtained. Calculating the mean and standard deviations by the strict definition encounters the problems described previously, but often noise and other effects make calculating the strict standard deviation and mean meaningless when trying to determine the average number of photoelectrons. Most of the time values are obtained by fitting the data with a Gaussian, wherever the data is considered to be meaningful. This introduces another problem. The trailing side of the spectrum (above the mean) is most often the easiest to fit with a Gaussian due to the fact that there tends to be less noise in this portion of the spectrum. However, the distribution should be a Poisson distribution, not a Gaussian. The falling side of a Poisson distribution is not as steep as a Gaussian, so the value for the standard deviation obtained is greater, again leading to a lower number of predicted photoelectrons. This error is usually the greatest source of disagreement between the actual average number of photoelectrons and the predicted number.

The method of trying to determine the number of initial photoelectrons from Equation 11 should always be used with caution, keeping in mind the actual intention for the values of A and σ. Most often the only practical way to extract a mean and standard deviation from a charge spectrum is with a Gaussian fit, but this introduces errors as can be seen in Figure 33. If the fitting is done on the trailing side of the peak, the resulting number can always be assumed to be lower than the real number of photoelectrons. Figure 34 shows the relative range of the distribution used to fit the Gaussian. The relationship between the mean and standard deviation of the Gaussian fit and the actual number of photoelectrons was found to be given by:

$$N \approx 1.6 \left(\frac{A}{\sigma}\right)^2 \tag{13}$$

The number of photoelectrons is given by N, and the mean and standard deviation of the Gaussian fit are given by A and σ, respectively. This coefficient is only correct between 10 and 15 photoelectrons. As the mean of the Poisson increases, the distribution can be described by a Gaussian. At large numbers of photoelectrons the coefficient tends towards one. The coefficient is also dependent on the standard deviation of the single photoelectron peak. As shown previously, the width of this peak, when summed

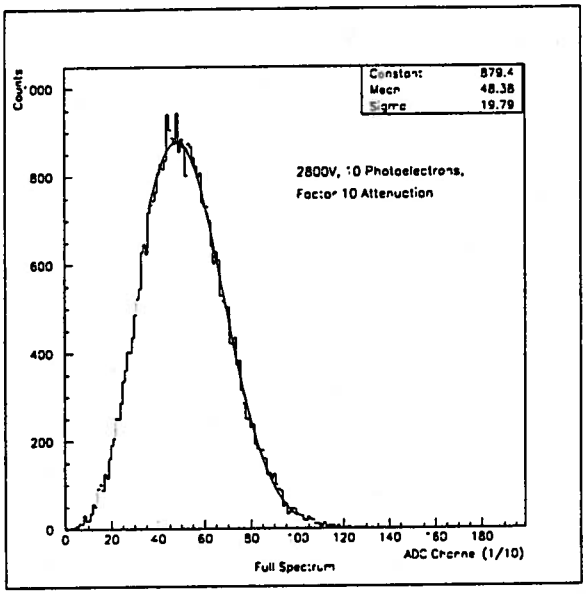

Figure 34: Example of Gaussian Fit of Distribution

with the others, contributes to the width of the entire distribution. Therefore, it is possible that the coefficient could differ for different phototubes or different base wiring schematics, as such changes could change the width of the single photoelectron peak.

7.4.2 Method Based on the Single Photoelectron Spectrum

There is another method for finding the number of photoelectrons which is more reliable. First the mean of the single photoelectron peak must be determined for a particular voltage. This can be done from actual data or a Monte Carlo simulation (if the gain is correctly modeled). Then, the fractional shift of the mean of the single photoelectron spectrum due to the tail must be determined, which for the experiment followed Equation 12. Then the mean of the distribution with unknown average number of photoelectrons is determined by Gaussian fitting. The ratio of the mean of the distribution to the corrected mean of the single photoelectron distribution should then be the average number of photoelectrons, but another correction must be made for the Poisson distribution. When the mean of a Poisson distribution is an integer, it is easy to show that the values with the highest probability of occurring are the mean and one less than the mean. If the Poisson distribution was continuous, the extremum would fall somewhere

Photoelectrons	Voltage (V)	$N_{Predicted}$
$N = 1.6(A/\sigma)^2$		
10	2800	8.99
	2400	9.97
15	2800	15.10
	2400	15.68
$N = A_{Dist}/(0.80A_{1PEPeak}) + 0.5$		
10	2800	9.74
	2400	9.97
15	2800	14.81
	2400	15.04

Figure 35: Table Comparing Predicted and Actual Number of Photoelectrons

between those two values. The extremum was approximated to be in the middle. When the peak of the distribution is fit, this fact must also be taken into account. The relationship with all corrections is given by:

$$N \approx \frac{A_{Distribution}}{0.80A_{1PEPeak}} + 0.5 \tag{14}$$

The number of photoelectrons is given by N, the mean of the entire distribution is given by $A_{Distribution}$, and the mean of the single photoelectron peak (excluding the tail) is given by $A_{1PEPeak}$.

Figure 35 shows a comparison of the accuracy of the methods described in Equations 13 and 14 for finding the number of initial photoelectrons from Gaussian fit data. The method in Equation 14 is a bit more stable, due to the lack of dependence on the standard deviation of the entire distribution which can vary significantly depending on how the spectrum is fit to a Gaussian function.

7.5 Efficiency and Threshold

The Monte Carlo simulation was also used to investigate the effect of different threshold settings on efficiency of detection of photons. The simulation has the ability to set a threshold in bins (2.5 pC / Bin), and all points below this threshold are dropped. The simulation was modified to keep track of how many events out of the total fell below the threshold. The simulation was run using a pure Poisson distribution, a Gaussian shape for the single

Thresh	Poisson Theory	Poisson Meas	Gauss	Actual
$0.25A_1$	$P_0 = 4.5 \times 10^{-5}$	4.3×10^{-5}	5×10^{-5}	1.3×10^{-4}
$0.5A_1$	$P_0 = 4.5 \times 10^{-5}$	4.3×10^{-5}	5×10^{-5}	2.3×10^{-4}
$1.5A_1$	$P_0 + P_1 = 5 \times 10^{-4}$	5.1×10^{-4}	4.6×10^{-4}	2.0×10^{-4}
$2.5A_1$	$P_0 + P_1 + P_2 = 0.0028$	0.0028	0.0031	0.011

Figure 36: Table Showing Fraction of Events Under Threshold, 10 Photoelectron Average

photoelectron peak, and also the Gaussian and tail for the single photoelectron distribution.

For a Poisson distribution, the number of events below threshold should be equal to the sum of the probabilities of all values of n (Equation 10) below the threshold multiplied by the number of events. These probabilities were calculated and compared with results from the Monte Carlo simulation. The table in Figure 36 shows a summary of the data for this experiment. The data was taken at 2600 V with an average of ten photoelectrons. The threshold was set halfway between integer multiples of the peak of the single photoelectron distribution, and also a run at one quarter of the mean of the single photoelectron peak was done only for the Gaussian distribution with the tail. The threshold setting is indicated in the column *Thresh*, where A_1 represents the mean of the single photoelectron peak (not including the tail). The column *Poisson Theory* shows the probability calculated from the Poisson distribution, where P_i represents the $P(i, A)$ in Equation 10. The column *Poisson Meas* shows values of the probability measured from simulations with a pure Poisson distribution. The column *Gauss* shows the probabilities for a simulation with a Gaussian distribution for one photoelectron. The probabilities found by running a simulation with the Gaussian and tail for the single photoelectron distribution are shown in the column labeled *Actual*.

The predicted and measured probabilities for the Poisson distribution agree very well. The probabilities measured for the Gaussian are also in agreement with the predicted values. However, the probabilities found by using the model for the actual single photoelectron distribution are larger than predicted, and can be significant. By a threshold at $\frac{5}{2}A_1$, more than one percent of the events are found to be below threshold. The effect of threshold on efficiency is greater for the actual distribution than for a pure Poisson distribution.

8 Summary

8.1 Conclusions as a Result of Experimental Work

Several things can be concluded from this investigation of the BURLE 8854 Photomultiplier tube.

- The single photoelectron spectrum is described by more than a Gaussian distribution about the average pulse charge for a single photoelectron entering the dynode chain from the photocathode. The single photoelectron spectrum also includes a tail of events which are lower in charge than the typical single photoelectron. The shape of this tail appears to be relatively stable over the operating range of the phototube, and approximately 20% of the spectrum appears to fall in the tail.

- When considering events aboved a fixed threshold, increasing voltage produces a definite increase in efficiency. This increase is due to the fact that with each increase in voltage more low charge events (resulting from the elastic collision of a photoelectron with the first dynode) are included in the analysis.

- When considering events above a fixed relative threshold, such as the number of events under the single photoelectron peak of an ADC spectrum, and using a green LED as a photon source, the efficiency is relatively constant with voltage. However, by increasing the field between the photocathode and the first dynode by a factor of 2, the probability that the initial photoelectron will undergo an elastic collision with the first dynode and rebound without producing further electrons on the first dynode is reduced. This leads to a slight, but noticeable ($\approx$4.5%), increase in the number of events under the single photoelectron spectrum.

- When the phototube is tested with actual Cherenkov radiation, which is concentrated in the ultra-violet portion of the spectrum, and events are considered above a fixed relative threshold, increasing the supply voltage from 2500 V to 2900 V produces an increase in efficiency of approximately 4.5%. This increase in efficiency does not appear to depend on where the incident photon strikes the photocathode.

- The current phototube base (Figure 13) is suitable for applications which require charge linearity up to 700 pC. If necessary, higher charge

linearity, up to 3000 pC, can be achieved by progressively increasing the values of the resistors between the last few dynodes (as shown in Figure 22).

- After exposure to light, the dark noise in the phototube decays rapidly when voltage is applied to the tube. In in approximately 12 minutes, the frequency of dark pulses was reduced by a factor of 10 when 2900V was applied to the phototube after photocathode exposure.

8.2 Suggestions for Base Modification

The wiring schematic for the base shown in Figure 13 is satisfactory as long as the application does not require that the base be linear for pulse charges over 700 pC. If higher charge linearity is necessary the resistor chain can be modified in the manner discussed in Section 4.3.3. This modification provides charge linearity for pulses up to at least 3000 pC. It is important that the resistive divider current (I_d) remains large with respect to the mean anode current (I_a). This is discussed in Section 4.3.4. This effect should be considered when dealing with high pulse rates (above 20 kHz) or periods during which high current will be applied to the anode for more than a quick (< 100 ns) pulse. If higher divider current (I_d) is desired, the suggested resistor values can all be decreased by the same fraction. This should be done with caution as lower overall resistance will increase the current drawn from the supply, and increase the the heat dissipation by the resistors ($P = I^2R$). It can also be concluded that increasing the cathode to dynode resistance to $600k\Omega$ produces a slight, but noticeable, increase in efficiency. Finally, the 500Ω resistor at the anode has been shown to have little effect on the pulse size. Based on these conclusions, the suggested wiring schematic for high charge linearity is shown in Figure 37.

8.3 Suggestions for Data Analysis

Several considerations must be taken into account when trying to use the charge spectrum from a phototube to try and determine the average number of initial photoelectrons. Corrections must be made for properties of the Poisson distribution of initial photoelectrons, the amplitude distribution of the single photoelectron spectrum, and the fact that most data will be collected from a Gaussian fit of the upper portion of the spectrum. Two methods have been compared (those described by Equations 13 and 14), and it has been determined that it is more consistent to use a method that does not depend on the standard deviation of the Gaussian fit because of

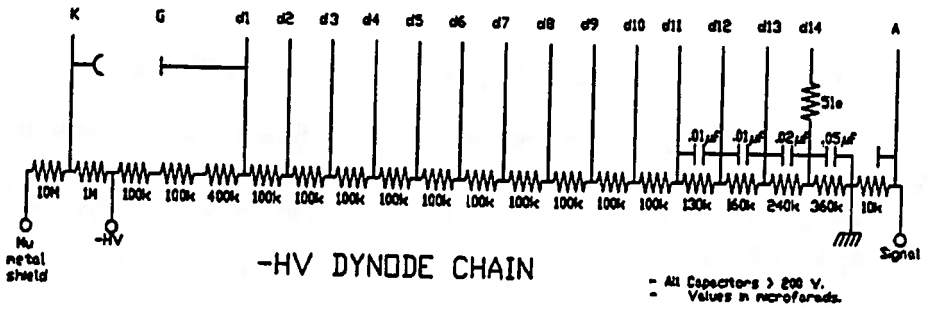

Figure 37: Suggested Wiring Schematic for Base

the instability of this quantity. Therefore, the method described in Equation 14 is recommended for most applications. This method is based off the actual mean of the single photoelectron distribution. It has been concluded that this technique of analysis is the most stable and also the least likely to affected by extra noise in the charge spectra. When the actual mean of the single photoelectron spectrum can not be determined, it is best to approximate this value as 80% of the mean of the single photoelectron peak (Equation 12).

A Monte Carlo Simulation C++ Source Code

This source code was compiled and run on a Sun Sparc Ultra170 running Solaris 2.5. The GNU C compiler gcc version 2.7 was used by calling g++ so that the C++ code would be recognized. The code (named spectrum.cc) was compiled with the command:

g++ -o spectrum spectrum.cc

The math.h library must be linked in order for the program to successfully run. This may require the -lm option on some systems.

The minimum information needed to run the program is input as:

spectrum *voltage attenuation photoelectrons*

The total supply voltage is given by *voltage*. The attenuation of the photomultiplier signal is given by *attenuation*, and is equal to the factor by which the signal is to be divided. The average number of photoelectrons ejected by the photocathode is given by *photoelectrons*. More options are available by entering a non-zero number after the other command line parameters. The user is then prompted for a threshold setting (default is zero), which is multiplied by ten to get the ADC channel for the cutoff (the multiplication by ten is convenient because the data output by the program was rebinned by a factor of ten before being analyzed). The user is then prompted for a gain factor (default is zero) to fit the program to individual 8854 tubes because the have different gains. The gain factor is given in percent divided by ten by which the gain is to be scaled, for example an input of 10 increases the simulated gain by 100% and an input of -1 decreases the gain by 10%.

A directory called "newspec" must be created as a subdirectory of the directory in which the program is run before running the program. All output files are put in this directory. Each run of the program results in 31 files. The format of the file names is:

voltage_attenuation_photoelectrons_number

The last part of the file name indicates the number of initial photoelectrons represented in that particular histogram file. The file ending in 0 is the sum of all other histograms, the spectrum actually seen if the experiment was run. The histograms for specific numbers of initial photoelectrons were created to analyze the effect of the algorithm used to simulate the low

charge events on larger numbers of photoelectrons and to look at the relations between mean and standard deviations of the individual peaks without interference from other peaks. The output of the program can be analyzed in any program that can import text and make histograms. The file format is one channel per line (200 channels at 2.5 pC per channel).

```
#include <iostream.h>
#include <fstream.h>
#include <stdlib.h>
#include <sys/types.h>
#include <time.h>
#include <math.h>
#include <String.h>

//DEFINES

//number of bins (in x direction)
#define BINS 200

//maximum number of photoelectrons considered
#define MAX_PE 30

//how many events to simulate
#define NUM_EVENTS 40000

//FUNCTION PROTOTYPES

//return a random integer between lower and upper
int myRandInt(int lower, int upper);

//return a random double between lower and upper
double myRandDouble(double lower, double upper);

//return the value of the poisson distribution with
//average value at x
double myPoisson(int x, double avg);

//return value of gauss distribution with mean,
//standard deviation  at x
```

```
double myGauss(double x, double mean, double stdev);

//return x! (return is a double to be able to handle
//large numbers)
double factorial(int x);

//return a random value conforming to a poisson
//distribution
int poissonBin(double avg, int xMax, double yMax);

//return a random value conforming to a gauss
//distribution
double gaussBin(double mean, double stdev, double lc);

//calculates unattenuated mean from voltage
double myMean(double voltage);

//calculates unattenuated stdev from voltage
double myStdev(double voltage);

//calculates low charge events for a gauss with mean
double myLowC(double mean);

//returns the value attenuated by att
double myAtt(double value, double att);

//Converts an integer to a String
String myIntToString(int x);

//Converts a double to string, accurate to tenths place
String myTenthsToString(double x);

//Converts a String to a double
double myStringToDouble(String num);

//for optimization calculates the highest x value to
//guess in the poisson
int maxPoissonX(double avg);

//for optimization calculates the highest y value to
```

```
//guess in the poisson
double maxPoissonY(double avg);

//rounding integer routine
int myRound(double x);

//MAIN

/*This is the main part of the program.  There are 3
 required command line parameters and one optional.
 They are [voltage] [attenuation] [average number of
 photoelectrons] [editor mode (non zero value)](opt.)
 If the last parameter is omitted a default value of
 zero is used.
  */

void main(int argc, char *argv[]) {
  if(argc < 4) {
    cerr << "Error: too few parameters\n";
    exit(-1);
  }

  srand48(time(NULL));

  /*make 2 D array to hold all of the info to be written
    to files (spectra) there are MAX_PE+1 different spectra
    (one for the combined spectra) and each has BINS number
    of bins
    */

  int spectra[MAX_PE+1][BINS];
  for(int i=0; i<MAX_PE+1; i++)
    for(int j=0; j<BINS; j++)
      spectra[i][j]=0;

  /*
    gf is gain factor, gain factor scales the average and
    stdev. linearly in an attempt to account for variations
    in the gain of the tubes.
  */
```

```
double voltage, att, avgpe, opt;

opt=0;

voltage = myStringToDouble(argv[1]);
att = myStringToDouble(argv[2]);
while(att <= 0) {
  cout << "Please enter a positive attenuation factor: ";
  cin >> att;
}
avgpe = myStringToDouble(argv[3]);

if(argc > 4)
  opt=myStringToDouble(argv[4]);

double thresh=0,gf=0;

if(opt !=0){
  cout << "\n***Entering Option Editing Mode***\n\n"
<< "Enter the threshold (ADC Channel/10)(default=0):";
  cin >> thresh;
  cout << "Enter the gain factor(default=0):";
  cin >> gf;
}

double stdev = myStdev(voltage);
double mean = myMean(voltage);
int poissonX = maxPoissonX(avgpe);
double poissonY = maxPoissonY(avgpe);

/*adjust mean and stdev*/

mean = mean + gf*mean;
stdev = stdev + 0.34*gf*stdev;

/*get Low Charge Fraction before mean is attenuated*/

double lc=myLowC(mean);
```

```
/*attenuate mean and stdev*/

mean=myAtt(mean,att);
stdev=myAtt(stdev,att);

for(int i=0; i<NUM_EVENTS;) {

  int numPE = poissonBin(avgpe, poissonX, poissonY);

  double tmpGauss=0.0;
  for(int j=0; j<numPE; j++) {
    tmpGauss += gaussBin(mean,stdev,lc);

  }

  if(tmpGauss>=thresh) {
    int gauss = myRound(tmpGauss);
    if(gauss > BINS-1)
      gauss=BINS-1;
    spectra[numPE][gauss]++;
    i++;
  }
}


for(int i=0; i<BINS; i++)
  for(int j=1; j<MAX_PE+1; j++)
    spectra[0][i] += spectra[j][i];


//output is "newspec/[voltage]_[attenuation]_[avgPE]"
//all to tenths place

for(int i=0; i<MAX_PE+1; i++) {
  ofstream file_out;
  String name;
  name = "newspec/";
  name += myTenthsToString(voltage);
  name += "_";
  name += myTenthsToString(att);
```

```
    name += "_";
    name += myTenthsToString(avgpe);
    name +="_";
    name += myIntToString(i);
    file_out.open(name);

    for(int j=0; j<BINS; j++)
      file_out << spectra[i][j] << endl;
    file_out.close();
  }

}


int myRandInt(int lower, int upper) {
  int done=0;
  int result;
  while(!done) {
    result = int((upper+1-lower)*drand48() + lower);
    if(result != upper+1)
      done=1;
  }
  return result;
}


double myRandDouble(double lower, double upper) {
  return (upper-lower)*drand48() + lower;
}

double myPoisson(int x, double avg) {
  return pow(avg,x)*exp(-avg)/factorial(x);
}

double myGauss(double x, double mean, double stdev) {
  return exp(-0.5*pow((mean-x)/(stdev),2));
}

double factorial(int x) {
  double result=1;
```

```
    for(int i=x; i>1; i--)
      result = result*i;
    return result;
  }

  int poissonBin(double avg, int xMax, double yMax) {
    int done=0;
    int x;
    while(!done) {
      double y = myRandDouble(0,yMax);
      x = myRandInt(0,xMax);
      if(y < myPoisson(x,avg))
        done=1;
    }
    return x;
  }


  double gaussBin(double mean, double stdev, double lc) {
    int done=0;
    double x;
    while(!done) {
      double y = myRandDouble(0,1);
      x = myRandDouble(0,mean+6*stdev);

      if((x<mean) && (y<lc))
        done=1;

      if(y < myGauss(x,mean,stdev))
        done=1;
    }
    return x;
  }

  //fit from data
  double myMean(double voltage) {
    return exp(0.00379*voltage-6.45);
  }

  //fit from data
```

```
double myStdev(double voltage) {
  return exp(0.0034*voltage-7.05);
}

//fit to data
double myLowC(double mean) {
  return (0.35 - 0.024*exp(0.0091*mean));
}

double myAtt(double value, double att) {
  return value/att;
}


String myIntToString(int x) {
  String result;

  if(x/10==0) {
    result = char('0'+x);
  }
  else {
    result = myIntToString(x/10);
    result += char('0' + x%10);
  }
  return result;
}


String myTenthsToString(double x) {
  int tmp = int(x*10);
  String result = myIntToString(tmp);
  char last = result[result.length()-1];
  result[result.length()-1]='.';
  result += last;
  return result;
}

double myStringToDouble(String num) {
  int decimalq=0;
  int power=-1;
```

```
    double result=0;
    for(int i=0; i<num.length(); i++) {
      if(num[i]=='.')
        decimalq=1;
      else if(!decimalq)
        result=10*result + double(num[i]-'0');
      else {
        result=result + double(num[i]-'0')*pow(10,power);
        power--;
      }
    }
    return result;
}

int maxPoissonX(double avg) {
    double maxY = maxPoissonY(avg);
    int i=0;
    for(i = int(avg)+1; (myPoisson(i,avg) > 0.001*maxY)
     && (i<MAX_PE); i++);
    return i;
}


double maxPoissonY(double avg) {

    int tmp = int(avg);
    double max = 0.0;
    int i=tmp-1;

    if(i < 0)
      i=0;
    for(i; i<=tmp+1; i++)
      if(myPoisson(i,avg) > max)
        max = myPoisson(i,avg);
    return max;
}

int myRound(double x) {
    int result = int(x);
    if( (x - result) > 0.5 )
```

```
    result++;
  return result;
}
```

B KUMAC File for Displaying Data From Monte Carlo Simulation in PAW

In order to display the data generated in the Monte Carlo Simulation, the following KUMAC file should be created. The simulation will output all of the files to a directory titled "newspec." Another directory titled "oldspec" must be created in the directory in which "newspec" resides. This KUMAC file should also be in the directory in which "newspec" and "oldspec" reside. PAW should be started from this directory (the one with the KUMAC file and directories "newspec" and "oldspec"). When the KUMAC file is executed, it will import all of the data into histograms. As the data is being read in, it will be moved from the "newspec" to the "oldspec" directory. The plot of the Full Charge spectrum for the parameters specified in the initial running of the Monte Carlo Simulation will reside in histogram ID# 31 and will be plotted automatically. The contributions of all of the individual spectra, from 1 to 30 photoelectrons, can also be viewed by plotting the histogram with the ID# that corresponds to the particular number of photoelectrons.

```
vec/create 1(200) I
vec/create 2(200) I
vec/create 3(200) I
vec/create 4(200) I
vec/create 5(200) I
vec/create 6(200) I
vec/create 7(200) I
vec/create 8(200) I
vec/create 9(200) I
vec/create 10(200) I
vec/create 11(200) I
vec/create 12(200) I
vec/create 13(200) I
vec/create 14(200) I
vec/create 15(200) I
vec/create 16(200) I
vec/create 17(200) I
vec/create 18(200) I
vec/create 19(200) I
vec/create 20(200) I
vec/create 21(200) I
```

```
vec/create 22(200) I
vec/create 23(200) I
vec/create 24(200) I
vec/create 25(200) I
vec/create 26(200) I
vec/create 27(200) I
vec/create 28(200) I
vec/create 29(200) I
vec/create 30(200) I
vec/create 31(200) I
sh cp newspec/*_1 temp
vec/read 1 temp
sh mv newspec/*_1 oldspec/
sh cp newspec/*_2 temp
vec/read 2 temp
sh mv newspec/*_2 oldspec/
sh cp newspec/*_3 temp
vec/read 3 temp
sh mv newspec/*_3 oldspec/
sh cp newspec/*_4 temp
vec/read 4 temp
sh mv newspec/*_4 oldspec/
sh cp newspec/*_5 temp
vec/read 5 temp
sh mv newspec/*_5 oldspec/
sh cp newspec/*_6 temp
vec/read 6 temp
sh mv newspec/*_6 oldspec/
sh cp newspec/*_7 temp
vec/read 7 temp
sh mv newspec/*_7 oldspec/
sh cp newspec/*_8 temp
vec/read 8 temp
sh mv newspec/*_8 oldspec/
sh cp newspec/*_9 temp
vec/read 9 temp
sh mv newspec/*_9 oldspec/
sh cp newspec/*_10 temp
vec/read 10 temp
sh mv newspec/*_10 oldspec/
```

```
sh cp newspec/*_11 temp
vec/read 11 temp
sh mv newspec/*_11 oldspec/
sh cp newspec/*_12 temp
vec/read 12 temp
sh mv newspec/*_12 oldspec/
sh cp newspec/*_13 temp
vec/read 13 temp
sh mv newspec/*_13 oldspec/
sh cp newspec/*_14 temp
vec/read 14 temp
sh mv newspec/*_14 oldspec/
sh cp newspec/*_15 temp
vec/read 15 temp
sh mv newspec/*_15 oldspec/
sh cp newspec/*_16 temp
vec/read 16 temp
sh mv newspec/*_16 oldspec/
sh cp newspec/*_17 temp
vec/read 17 temp
sh mv newspec/*_17 oldspec/
sh cp newspec/*_18 temp
vec/read 18 temp
sh mv newspec/*_18 oldspec/
sh cp newspec/*_19 temp
vec/read 19 temp
sh mv newspec/*_19 oldspec/
sh cp newspec/*_20 temp
vec/read 20 temp
sh mv newspec/*_20 oldspec/
sh cp newspec/*_21 temp
vec/read 21 temp
sh mv newspec/*_21 oldspec/
sh cp newspec/*_22 temp
vec/read 22 temp
sh mv newspec/*_22 oldspec/
sh cp newspec/*_23 temp
vec/read 23 temp
sh mv newspec/*_23 oldspec/
sh cp newspec/*_24 temp
```

```
vec/read 24 temp
sh mv newspec/*_24 oldspec/
sh cp newspec/*_25 temp
vec/read 25 temp
sh mv newspec/*_25 oldspec/
sh cp newspec/*_26 temp
vec/read 26 temp
sh mv newspec/*_26 oldspec/
sh cp newspec/*_27 temp
vec/read 27 temp
sh mv newspec/*_27 oldspec/
sh cp newspec/*_28 temp
vec/read 28 temp
sh mv newspec/*_28 oldspec/
sh cp newspec/*_29 temp
vec/read 29 temp
sh mv newspec/*_29 oldspec/
sh cp newspec/*_30 temp
vec/read 30 temp
sh mv newspec/*_30 oldspec/
sh cp newspec/*_0 temp
vec/read 31 temp
sh mv newspec/*_0 oldspec/
his/create/1dhisto 1 '1 Photoelectron' 200 1 200
his/create/1dhisto 2 '2 Photoelectrons' 200 1 200
his/create/1dhisto 3 '3 Photoelectrons' 200 1 200
his/create/1dhisto 4 '4 Photoelectrons' 200 1 200
his/create/1dhisto 5 '5 Photoelectrons' 200 1 200
his/create/1dhisto 6 '6 Photoelectrons' 200 1 200
his/create/1dhisto 7 '7 Photoelectrons' 200 1 200
his/create/1dhisto 8 '8 Photoelectrons' 200 1 200
his/create/1dhisto 9 '9 Photoelectrons' 200 1 200
his/create/1dhisto 10 '10 Photoelectrons' 200 1 200
his/create/1dhisto 11 '11 Photoelectrons' 200 1 200
his/create/1dhisto 12 '12 Photoelectrons' 200 1 200
his/create/1dhisto 13 '13 Photoelectrons' 200 1 200
his/create/1dhisto 14 '14 Photoelectrons' 200 1 200
his/create/1dhisto 15 '15 Photoelectrons' 200 1 200
his/create/1dhisto 16 '16 Photoelectrons' 200 1 200
his/create/1dhisto 17 '17 Photoelectrons' 200 1 200
```

```
his/create/1dhisto 18 '18 Photoelectrons' 200 1 200
his/create/1dhisto 19 '19 Photoelectrons' 200 1 200
his/create/1dhisto 20 '20 Photoelectrons' 200 1 200
his/create/1dhisto 21 '21 Photoelectrons' 200 1 200
his/create/1dhisto 22 '22 Photoelectrons' 200 1 200
his/create/1dhisto 23 '23 Photoelectrons' 200 1 200
his/create/1dhisto 24 '24 Photoelectrons' 200 1 200
his/create/1dhisto 25 '25 Photoelectrons' 200 1 200
his/create/1dhisto 26 '26 Photoelectrons' 200 1 200
his/create/1dhisto 27 '27 Photoelectrons' 200 1 200
his/create/1dhisto 28 '28 Photoelectrons' 200 1 200
his/create/1dhisto 29 '29 Photoelectrons' 200 1 200
his/create/1dhisto 30 '30 Photoelectrons' 200 1 200
his/create/1dhisto 31 'Full Spectrum' 200 1 200
his/put_vec/contents 1 1
his/put_vec/contents 2 2
his/put_vec/contents 3 3
his/put_vec/contents 4 4
his/put_vec/contents 5 5
his/put_vec/contents 6 6
his/put_vec/contents 7 7
his/put_vec/contents 8 8
his/put_vec/contents 9 9
his/put_vec/contents 10 10
his/put_vec/contents 11 11
his/put_vec/contents 12 12
his/put_vec/contents 13 13
his/put_vec/contents 14 14
his/put_vec/contents 15 15
his/put_vec/contents 16 16
his/put_vec/contents 17 17
his/put_vec/contents 18 18
his/put_vec/contents 19 19
his/put_vec/contents 20 20
his/put_vec/contents 21 21
his/put_vec/contents 22 22
his/put_vec/contents 23 23
his/put_vec/contents 24 24
his/put_vec/contents 25 25
his/put_vec/contents 26 26
```

```
his/put_vec/contents 27 27
his/put_vec/contents 28 28
his/put_vec/contents 29 29
his/put_vec/contents 30 30
his/put_vec/contents 31 31
option stat
set stat 0000010
his/plot 31
```